Bellas CM, Anesio AMB, Telling J, Stibal M, Tranter M, Davis SA.

Viral impacts on bacterial communities in Arctic cryoconite.

***Environmental Research Letters* 2013, 8, 045021.**

Viral impacts on bacterial communities in Arctic cryoconite

2013 Environ. Res. Lett. 8 045021

(http://iopscience.iop.org/1748-9326/8/4/045021)

OPEN ACCESS
IOP PUBLISHING ENVIRONMENTAL RESEARCH LETTERS
Environ. Res. Lett. **8** (2013) 045021 (9pp) doi:10.1088/1748-9326/8/4/045021

Viral impacts on bacterial communities in Arctic cryoconite

Christopher M Bellas[1], Alexandre M Anesio[1], Jon Telling[1], Marek Stibal[2,3], Martyn Tranter[1] and Sean Davis[4]

[1] School of Geographical Sciences, University of Bristol, Bristol, UK
[2] Department of Geochemistry, Geological Survey of Denmark and Greenland (GEUS), Copenhagen, Denmark
[3] Center for Permafrost (CENPERM), University of Copenhagen, Copenhagen, Denmark
[4] School of Chemistry, University of Bristol, Bristol, UK

E-mail: chris.bellas@bristol.ac.uk

Received 12 April 2013
Accepted for publication 2 October 2013
Published 30 October 2013
Online at stacks.iop.org/ERL/8/045021

Abstract
The surfaces of glaciers are extreme ecosystems dominated by microbial communities. Viruses are found in abundance here, with a high frequency of bacteria displaying visible virus infection. In this study, viral and bacterial production was measured in Arctic cryoconite holes to address the control that viruses play in these highly truncated ecosystems. Mean bacterial carbon production in the sediments of cryoconite holes was found to be 57.8 ± 12.9 ng C g^{-1} dry wt. h^{-1}, which predicted a mean of 1.89–5.41 × 10^6 cells g^{-1} dry wt. h^{-1} based on a range of conversion factors. Relative to this, virus production was found to be high, up to 8.98 × 10^7 virus like particles g^{-1} dry wt. h^{-1} were produced, which is comparable to virus production in sediments around the globe. The virus burst size was assessed by transmission electron microscopy and found to be amongst the lowest recorded in the literature (mean 2.4). Hence, to account for the measured virus production, the viral induced bacterial mortality was calculated to be more than capable of accounting for the mortality of all bacterial production. The data presented here, therefore, suggests that viral induced mortality is a dominant process for the release and recycling of carbon and nutrients in supraglacial ecosystems.

Keywords: virus, bacteriophage, cryoconite, glacier, DOM

S Online supplementary data available from stacks.iop.org/ERL/8/045021/mmedia

Non-standard abbreviations

BDC	Bacterial direct counts
BCP	Bacterial carbon production
B_z	Burst size
CC	Carbon content ($cell^{-1}$)
FVIC	Frequency of visibly infected cells
GrIS	Greenland ice sheet
NCP	New cell production
VBR	Virus to bacteria ratio
VIBM	Virus induced bacterial mortality (VMM ÷ NCP × 100)
VLP	Virus like particles
VMM	Virus mediated mortality (VP ÷ B_z)
VP	Virus production
VT	Virus turnover (VP ÷ VLP)

1. Introduction

Sedimentary ecosystems contain highly abundant virus communities which require high rates of new virus production to be maintained (Danovaro *et al* 2008a). In freshwater and marine sediments around the globe, virus production rates

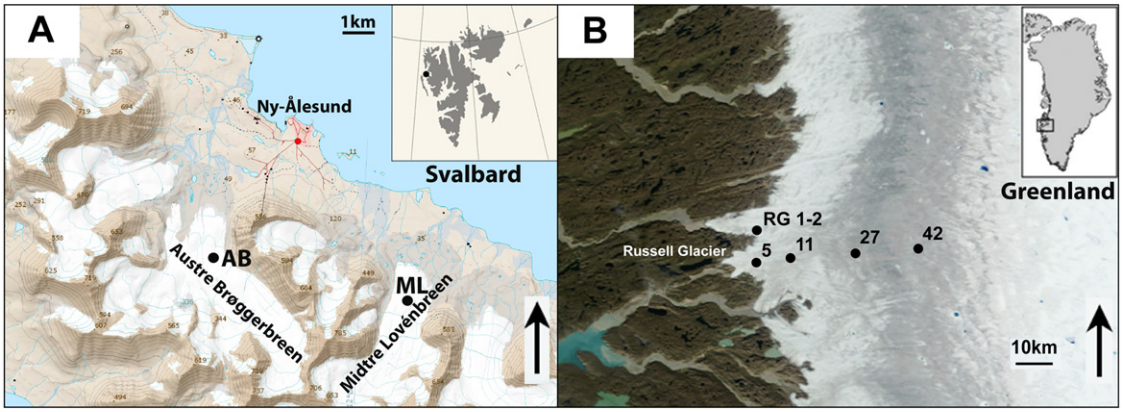

Figure 1. Map of sampling sites on Austre Brøggerbreen and Midtre Lovénbreen (A) around Ny-Ålesund (78.53°N 12.04°E), in the northwest of the Svalbard archipelago (courtesy of the Norwegian Polar Institute). Locations sampled on the Greenland ice sheet (B), numbers are distance in km from the ice sheet margin where cryoconite holes were sampled. Site RG1 and 2 were used in viral activity measurement. True colour MODIS image acquired 17 August 2010, NASA.

of 0.2–19.8 $\times$ 10^7 virus like particles (VLP) g^{-1} h^{-1} have been reported (Danovaro *et al* 2008a, 2008b). Such large scale virus production comes at a significant cost to heterotrophic bacterial hosts, as viral release from infected cells is generally via lysis. Lysis also releases cellular carbon and nutrients back into the dissolved and bioavailable particulate phase, effectively diverting the flow of carbon away from higher trophic levels, whist maintaining its availability for the remaining microbial community (Wilhelm and Suttle 1999). Viruses play a significant role in the carbon and nutrient transformations in sedimentary ecosystems. Between 10% and 100% of all bacterial carbon production is channelled through viral processes (Danovaro *et al* 2008a and references therein).

The surfaces of glaciers are extreme environments, characterized by persistent low temperatures, yet they harbour abundant communities of microorganisms which cycle carbon and nutrients (Stibal *et al* 2012a). The most abundant and active microbial communities are found in the small, water filled depressions known as cryoconite holes (Hodson *et al* 2008). Cryoconite is dark material on glacial ice that may arrive from the surrounding moraines, tundra, bed of the glacier (Wharton *et al* 1985, Fountain *et al* 2004, Hodson *et al* 2010), or may even be produced *in situ* by carbon fixation (Anesio *et al* 2009). The dark colouration of the material causes it to melt into the ice maintaining a pool of water above. Cryoconite holes are typically tens of cm wide and deep, with water temperatures relatively constant at ~0.1 °C (Säwström *et al* 2002). Cyanobacteria account for the majority of carbon fixation (Stibal *et al* 2006) and primary production is approximately balanced by respiration rates, depending on sediment depth (Telling *et al* 2012). However, bacterial production only accounts for <10% of the respiration values (Hodson *et al* 2007, Anesio *et al* 2010). In a previous study, bacterial production was not correlated to bacterial biomass, suggesting a strong top-down control on heterotrophic bacterial abundances in cryoconite holes (Anesio *et al* 2010). Grazers, such as ciliates and tardigrades, are present (Sømme 1996, Porazinska *et al* 2004), but their abundances are relatively low (Säwström *et al* 2002), suggesting an alternative control on bacterial abundances.

Viruses are likely to be important entities in cryoconite holes, responsible for a significant portion of heterotrophic bacterial mortality (Säwström *et al* 2007, Anesio *et al* 2007). The viral induced destruction of host cells and the release of cellular carbon and nutrients may be important for the continued production of the non-infected microbial community. Whether microbial communities and organic carbon build up on glaciers or are washed out to hydrologically connected ecosystems remains an important question. DOC in supraglacial runoff is believed to be derived, in part, from *in situ* microbial processes (Hood *et al* 2009). As a significant proportion of organic carbon may flow through viral mediated processes, there is a pressing need to investigate the impact of viruses on microbial communities and their potential to influence carbon cycling in these environments. In this study, the viral communities in the sediment of cryoconite holes are addressed. Here, virus abundances have been shown to be over an order of magnitude higher than the overlying waters (Anesio *et al* 2007) and the vast majority of microbial activity on a glacier takes place here. For the first time, rates of virus production are calculated and related to bacterial activity, allowing for the impact of viruses on the heterotrophic bacterial community to be estimated.

2. Methods

2.1. Study area and sample collection

This study addressed viral dynamics in cryoconite holes over two consecutive field seasons in Svalbard and Greenland. The Svalbard study centred on two valley glaciers, Midtre Lovénbreen (ML) and Austre Brøggerbreen (AB), near Ny-Ålesund (78°55′N 11°55′W, figure 1). Virus and bacterial production was measured in incubation experiments on the 25 July 2009 on sediment sampled from cryoconite holes at point ML, and on the 4 August 2009 from site AB

(figure 1). Between June and August 2010, sampling and activity measurements were conducted on the western margin of the Greenland ice sheet (GrIS) around Kangerlussuaq. The study sites for activity measurements were approximately 1 km from the ice margin on the Russell Glacier (RG) at approximately 67°9′39.7″N, 50°0′52.7″W (figure 1). Viral production was measured in two independent cryoconite holes at RG1 on 15 June 2010 and three independent cryoconite holes on 27 July 2010 at RG2 (figure 1 and table 1). A transect was also conducted via helicopter on 2 August 2010 to measure virus and bacterial abundances throughout the entire ablation zone of the GrIS (sample points 5–42 km); (figure 1). These points represented elevations of ∼550 m above sea level at point RG1 to 1186 m above sea level at 42 km.

2.2. Virus and bacterial counts

For enumeration of viruses and bacteria, 1 ml of cryoconite was sampled with a large pipette and transferred into a sterile 15 ml centrifuge tube. The sample was mixed with 9 ml of 30 kDa glacial ultrafiltrate which had a virus concentration of at least four orders of magnitude lower than the sediment and is hence referred to as virus-free water. This was shaken vigorously for 2 min. Fifteen seconds after cessation of shaking, 100 μl of supernatant was sampled and fixed with glutaraldehyde (2% final conc.), which allowed us to detect viruses at concentrations of 10^6 VLP g^{-1} or greater in this instance. Samples were filtered onto 0.02 μm Anodisc filters (Whatman) within 24 h, stained with SYBR gold (Invitrogen) and counted using epifluorescence microscopy (Anesio *et al* 2007). Bacterial biovolume was also calculated by measuring approximately 2000 individual bacteria from six cryoconite holes (three from RG1, two from ML, one from AB) using an F-view II CCD (Olympus) and digitally measuring the length (L) and width (W) using Cell^f software (Olympus) of bacteria in three fields of view per cryoconite. Cell biovolume (V) was calculated by using the formula $V = (\pi/4)W^2\left(L - \frac{W}{3}\right)$. The mean biovolume from the six cryoconites was used in further calculations. Biovolume (μm^3) was subsequently converted to carbon content (CC; fg $cell^{-1}$) by using a range of suitable conversion factors in the literature. Based on a review by Posch *et al* (2001) we chose CC conversion factors that are in common use in the literature and had been derived from freshwater bacteria and tested on the size range of bacteria present in cryoconite holes. This created a range of conversion factors from $CC = 105V$ (Theil-Nielsen and Søndergaard 1998) to $CC = 218V^{0.86}$ (Loferer-Krößbacher *et al* 1998).

2.3. Determination of burst size by TEM

1 ml of cryoconite from six cryoconite holes (three from RG1, two from ML, one from AB) was diluted with 9 ml of extraction buffer (2% glutaraldehyde, 10 mM sodium pyrophosphate and Milli-Q^{TM} water to 9 ml). The mixture was subjected to three cycles of vortexing and sonication for one minute, before it was passed through a 3 μm mixed cellulose ester filter (SSWP Millipore). To further separate the bacteria from the sediment matrix, a 200 μl aliquot of the filtered sediment extract was centrifuged onto a 70% sucrose cushion at 10 000 × g for 10 min. The top layer of this mixture, plus 100 μl from the top of the sucrose cushion, were removed and made up to 2 ml with 2% glutaraldehyde. This mixture was then pelleted at 10 000 × g for 5 min. The supernatant was removed and discarded before the pellet was resuspended in 1 ml 2% glutaraldehyde. The dilution step and further pelleting served to reduce the background level of viruses which remained in the supernatant. 5 μl of each sample was placed onto a carbon coated 400-mesh Cu grid resting on filter paper. Grids were left overnight to dry, before being negatively stained for one minute with 2% uranyl acetate and then rinsed with deionized distilled water. Two grids per cryoconite were examined for visibly infected bacterial cells at 80 kV and 20 000–40 000× magnification. A cell was considered infected when two or more viruses were visualized inside a cell based on a dark staining and a clearly recognizable round or hexagonal capsid structure. Normally, counting cells with such low numbers of virus particles inside increases the risk of counting cells that are simply resting on top of viruses as infected bacteria. This is because ultrafugation is the usual method to pellet both virus and host on to TEM grids (Bettarel *et al* 2006). In this study, the low speed centrifugation used to pellet bacteria, but not viruses, greatly reduced the free viruses. This allowed use of a lower detection limit of two phages per cell in a similar fashion to Säwström *et al* (2007). The frequency of infected cells (FVIC) and burst size (B_z) were calculated from the mean and standard deviation of the six cryoconite holes.

2.4. Virus production

Virus production (VP) was determined in cryoconite sediment samples using the dilution method (Mei and Danovaro 2004). A 1:10 sediment: virus-free water dilution was achieved for each of three sub-replicates per cryoconite hole in three holes from Svalbard and five from Greenland. Virus-free water (13.5 ml) was added to 1.5 ml cryoconite sediment to significantly reduce encounter rates and new virus infections. Each incubation was conducted for 24 h in the dark at *in situ* temperatures. To determine the virus increase, subsamples of 100 μl were removed at approximately 4 h intervals and immediately fixed with 0.02 μm-filtered glutaraldehyde (2% final conc.) before slide preparation and viral counts by epifluorescence microscopy as above. VLP were counted at each time point. VP was calculated by plotting a first order regression of VLP against time during the first increase in VLP numbers in each of the three sub-replicates. To confirm viruses were not simply detaching from the sediment and influencing counts, a killed control incubation was performed by adding glutaraldehyde (2% final conc.) to an extra replicate from each sample location and treated as above. All counts were normalized to dry weight by desiccation at 105 °C for 24 h.

To determine the significance of lysogeny in cryoconite holes, the induction agent mitomycin C was added to triplicate

Table 1. Mean virus and bacterial abundances and activity measurements calculated in cryoconite hole sediments from Svalbard and Greenland. (Note: all values are per g dry wt. sediment ± standard deviation of independent cryoconite holes except AB which is ± standard deviation of three replicates from the same cryoconite. VBR—virus to bacteria ratio; VIBM—virus induced bacterial mortality; VMM—virus mediated mortality).

Glacier	Position	Code	*n*	Date	Viruses (10^8 VLP g^{-1})	Bacteria (10^8 cells g^{-1})	VBR	Virus production (10^7 VLP g^{-1} h^{-1})	Virus turnover (h^{-1})	Bacterial production[a]		Bacterial turnover[a] (d^{-1})	VMM[b] (10^6 g^{-1} h^{-1})	VIBM[a,b] (%)
										(ng C g^{-1} h^{-1})	(10^6 Cells g^{-1} h^{-1})			
Midtre	78°53′25.57″N 12°3′16.32″E	ML	2	25/07/09	6.26 ± 0.90	3.99 ± 0.29	1.6	8.84 ± 0.20	0.143 ± 0.024	45.6 ± 14.36	1.49–4.27	0.089–0.255	36.8	911–2606
Austre	78°53′51.29″N 11°49′33.71″E	AB	1	01/08/09	7.52 ± 4.23	3.79 ± 0.27	2.0	8.17 ± 2.72	0.109 ± 0.071	48.6 ± 14.1	1.59–4.55	0.101–0.288	34.0	748–2139
Russell	67°9′39.71″N 50°0′52.66″W	RG1	2	15/06/10	13.5 ± 2.58	3.35 ± 0.23	4.0	6.38 ± 0.11	0.048 ± 0.004	72.7 ± 0.53	2.38–6.81	0.171–0.489	26.6	390–1115
Russell	67°9′39.20″N 50°0′52.76″W	RG2	3	27/07/10	8.23 ± 2.79	2.68 ± 0.00	3.1	4.87 ± 0.74	0.064 ± 0.021	64.2 ± 12.21	2.10–6.01	0.188–0.539	20.3	342–978
GrIS	67°5′34.70″N 50°1′8.90″W	5.4	3	02/08/10	23.2 ± 1.42	19.6 ± 1.34	1.2							
GrIS	67°6′15.40″N 49°48′26.60″W	11	3	02/08/10	24.5 ± 1.66	18.2 ± 2.87	1.3							
GrIS	67°6′56.70″N 49°24′5.20″W	27	3	02/08/10	20.4 ± 3.93	9.71 ± 1.42	2.1							
GrIS	67°7′36.40″N 49°0′36.00″W	42	3	02/08/10	14.4 ± 0.66	7.65 ± 0.67	1.9							
Mean					14.8 ± 7.3	8.62 ± 6.78	2.1	7.06 ± 1.80	0.091 ± 0.043	57.8 ± 12.9	1.89–5.41	0.137–0.393	29.4	598–1710

[a] Calculations are expressed as a range assuming 10.68–30.53 fg C bacterial $cell^{-1}$ calculated from mean cell biovolume of 0.102 μm^3 assuming a range of carbon conversion factors from $105V$ to $218V^{0.86}$ where $V = \mu m^3$ (Posch *et al* 2001).

[b] Calculation assumes a burst size of 2.4 from the TEM measurements and that all infections are lytic.

sediment dilutions as above to a final concentration of 1 μg ml^{-1}. Treatments were incubated for 24 h before a 100 μl subsample was removed, fixed and made into a slide, as described above. Triplicate incubations in which mitomycin C was not added, served as controls. The percentage of lysogenic bacteria was calculated according to Weinbauer and Suttle (1996).

2.5. Bacterial production

Bacterial carbon production (BCP) was measured alongside VP in each cryoconite hole ($n = 8$) by ^{3}H-leucine incorporation, modified from the method of Smith and Azam (1992) (see supplementary information 1, available at stacks.iop.org/ERL/8/045021/mmedia). Briefly nine 1.5 ml subsamples from each cryoconite hole were removed and transferred to sterile 1.7 ml microcentrifuge tubes. Incorporation was started by addition of ^{3}H-leucine (100 nM final conc.). Three of the tubes were incubated as killed controls by the immediate addition of 100 μl glutaraldehyde. The tubes (six live, three killed) were incubated at *in situ* temperature for 3 h and incorporation was stopped by addition of 100 μl glutaraldehyde (2% final conc.). BCP was converted to new bacterial cell production (NCP) by dividing BCP by the conversion factors calculated from the biovolume (10.68–30.53 fg C cell^{-1}) to produce a range of values.

2.6. Viral dynamics calculations

Viral turnover (VT) was calculated by dividing VP rates by initial viral abundances. The virus mediated mortality (VMM) of bacterial cells (cells lysed g^{-1} h^{-1}) was calculated by dividing VP values by the viral burst size (B_z). VMM was further divided by the NCP rate (cells g^{-1} h^{-1}), calculated from ^{3}H-leucine incorporation, to give a range of value for the virus induced bacterial mortality (VIBM) in each incubation expressed as a percentage of bacterial production.

2.7. Statistics

All data were tested for normality prior to statistical analysis using a Kolmogorov–Smirnov test conducted in SPSS (16.0) or SigmaPlot (12.0).

3. Results

3.1. Virus and bacterial abundances

Virus abundances in independent cryoconite holes in both Greenland and Svalbard ranged from 5.62 $\times$ 10^8 to 24.5 $\times$ 10^8 VLP g^{-1} dry weight sediment (ML and GrIS 11 km respectively), with a mean across all sites of 14.8 $\pm$ 7.3 $\times$ 10^8 VLP g^{-1} (table 1). Bacterial abundances ranged from 2.68 $\times$ 10^8 to 19.6 $\times$ 10^8 cells g^{-1} (RG2 and GrIS 5.4 km respectively), with mean abundances of 8.62 $\pm$ 6.8 $\times$ 10^8 cells g^{-1}. We can report that the coefficient of variation of VLP and BDC within cryoconite holes was generally less than 0.3, which was similar to the variation between cryoconite holes from the same site.

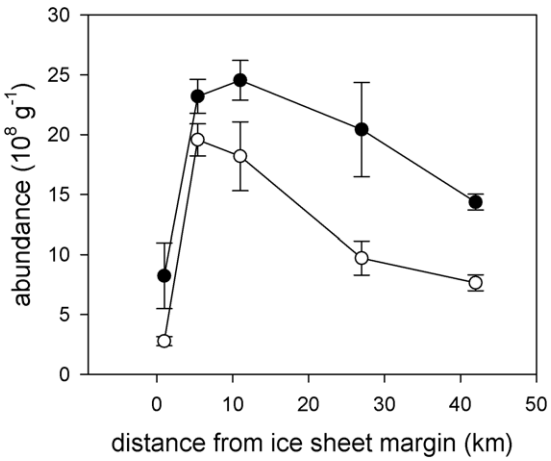

Figure 2. Virus like particle abundance (solid circles) and bacterial abundances (open circles) in cryoconite holes over a transect of the ablation zone of the Greenland ice sheet. Distances are from the nearest deglaciated point.

VLP and bacterial abundances were positively and significantly related across all sample sites (regression equation $y = 0.988x + 6.121 \times 10^8$, $n = 12$, $R^2 = 0.76$, $P < 0.001$) with a virus to bacteria ratio (VBR) between 1.2 and 4.4 (mean 2.1 $\pm$ 1). Over the 42 km transect of the ablation zone of the GrIS (figure 2), VLP abundances and BDC varied significantly (ANOVA, $P < 0.001$). Moving from the ice sheet margins to the interior, VLP abundances increased by a factor of three (ANOVA, $P < 0.001$ followed by post hoc Scheffé, $P < 0.001$) to a maximum at 11 km of 24.5 $\times$ 10^8 VLP g^{-1}. BDC also showed a seven fold increase between site RG (1 km) and their maximum at 5.4 km of 19.6 $\times$ 10^8 cells g^{-1} (ANOVA, $P < 0.001$, followed by post hoc Scheffé, $P < 0.001$). A planned 65 km site was also investigated but found to be above the snowline and insufficient cryoconite debris was obtained for counting.

For the purposes of comparing abundance variability, samples from Greenland were divided into outlet glacial locations and the ice sheet itself. Stibal *et al* (2012b) previously demonstrated that the marginal sites of the GrIS (<3.6 km from the margin) are physically and chemically different from the ice sheet interior because of their slope and proximity to deglaciated areas. Hence all cryoconite holes ($n = 5$) from sites RG1 and 2 (Greenland) (~1 km from the ice sheet margin) were considered part of the Russell Glacier (figure 1). Abundance data from 5.4 to 42 km on the transect across the GrIS ($n = 12$) were considered together as representative of the main ablation zone of the ice sheet and are subsequently referred to as GrIS sites. Cryoconite holes from ML and AB represented Svalbard cryoconite holes ($n = 3$). Using the above criteria, there were significant differences in VLP abundances between sites (ANOVA $P = 0.001$). GrIS VLP abundances (sites 5.4–42 km) were approximately 2–4 times greater than the glacial sites in Svalbard and Greenland (post hoc Scheffé,

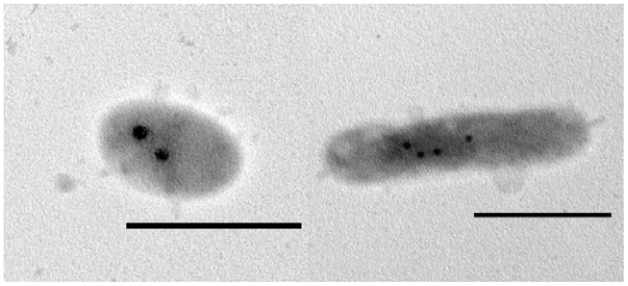

Figure 3. Transmission electron microscopy images of bacteria extracted from cryoconite hole sediment showing the minimum and maximum observed burst size of 2 and 4 viruses per cell. Cells were considered infected when two or more virus particles were visible. Scale bar represents 1000 nm.

$P < 0.01$). However, no significant differences were detected in VLP abundance between Svalbard and Greenland glacial sites (post hoc Scheffé, $P > 0.05$). Mean bacterial abundances were approximately 4 times greater on the main GrIS (Sites 5.4–42 km) than the Svalbard or Greenland glacial sites (ANOVA $P < 0.001$ followed by post hoc Scheffé, $P < 0.05$), but again no significant differences were found between Svalbard and Greenland glacial bacterial counts (post hoc Scheffé, $P < 0.05$).

3.2. Burst size

Visible virus infection in bacterial cells was clearly resolved using TEM (figure 3) by visualizing over 140 bacteria. Bacterial cells exhibited very low numbers of visible virus particles with a range of between 2 and 4 viruses per cell (mean 2.4 ± 0.5). No cells appeared replete with viruses. All viruses infecting bacteria were round or hexagonal in shape and were approximately 30–90 nm across. The frequency of visibly infected cells (FVIC) was calculated as $21 \pm 6\%$.

3.3. Virus and bacterial production

Rates of virus production (VP) in independent cryoconite holes ranged from 4.41×10^7 VLP g^{-1} h^{-1} (RG2) to 8.98×10^7 VLP g^{-1} h^{-1} (ML) with a mean of $7.06 \pm 1.8 \times 10^7$ VLP g^{-1} h^{-1} across all sites (table 1). No increase in VLP abundances was detected in the killed controls and lysogeny was also not detected in any of the mitomycin C incubations during the VP experiments. Viral turnover (VT) was calculated to range from 0.04 h^{-1} (RG2) to 0.16 h^{-1} (ML). Mean bacterial biovolume from cryoconite hole sediment was calculated to be 0.102 μm^3, thus the mean bacterial carbon content (CC) for cryoconite heterotrophic bacteria was calculated to range from 10.68 to 30.53 fg C $cell^{-1}$. Bacterial carbon production (BCP) in cryoconite holes ranged from 35.4 to 73.3 ng C g^{-1} h^{-1} (ML and RG2 respectively), (mean 57.8 ± 12.9 ng C g^{-1} h^{-1}). Using the CC conversion values BCP was equivalent to a mean new cell production (NCP) rate of $1.89–5.41 \times 10^6$ cells g^{-1} h^{-1}. Mean bacterial turnover, expressed as the ratio of NCP to bacterial abundance, ranged from 0.137 to 0.393 d^{-1}. VP was significantly related to bacterial abundance and could be predicted by the regression equation $y = 0.298x - 3.325 \times 10^7$ ($n = 8, R = 0.943$, $P < 0.005$). There was no significant correlation between bacterial production and virus production ($n = 8, R = 0.56$, $P > 0.05$), nor any correlation between bacterial production and bacterial abundance ($n = 8, R = 0.46$, $P > 0.05$). By using the burst size derived from TEM measurements, viruses were calculated to account for the mean abatement of 598%–1710% of the heterotrophic bacterial production across all sites (table 1).

4. Discussion

This study provides evidence that viruses are highly abundant and active components of cryoconite hole ecosystems, with the potential to significantly impact upon bacterial mortality and the cycling of organic carbon. Virus dynamics in cryoconite holes appear to proceed at rates comparable to other sedimentary ecosystems, despite the extreme conditions they inhabit. Virus abundances and production are similar to median values reported from both freshwater and marine global sediments (table 2; Danovaro *et al* 2008a, 2008b). The high rates of viral production measured in cryoconite holes results in a rapid mean viral turnover of 0.091 h^{-1}, which is also parallelled in marine sediments (mean 0.071 h^{-1}; Danovaro *et al* 2008b). These high rates of virus production may be key to maintaining viral numbers in supraglacial ecosystems in response to the continual destruction of viruses in by such factors such as UV-B radiation (Suttle and Feng 1992), extracellular enzymatic degradation and adsorption to sediment particles (Noble and Fuhrman 1997). Assuming lytic interactions, virus production must come at the detriment of a large number of host organisms. Whilst both cyanobacteria and algae are also subjected to viral infection, heterotrophic bacteria are usually the main hosts for viruses in the environment because of their numerical dominance. Cyanobacteria made up 0.5%–18.3% (mean 10.5%) of the total cell counts over a similar transect of the GrIS (Stibal *et al* 2012b), and $<0.8 \pm 1.4\%$ of the microbial community by abundance on four Svalbard glaciers (Stibal *et al* 2006). Hence, the most abundantly available hosts for viruses in cryoconite holes are heterotrophic bacteria. This is reinforced with TEM data which revealed that $21 \pm 6\%$ of the heterotrophic bacterial community displayed visible virus infection, meaning on average ~18% of the total virions in cryoconite sediments were intracellular at any one time. As visible infection only occurs in the latter stage of infection, the real infection rates are likely to be much greater. Concurrently, viral and bacterial abundances over all activity sites and across our Greenland transect were positively correlated, and virus production was strongly correlated with bacterial abundance, suggesting heterotrophic bacteria are the main virion production factories in cryoconite hole ecosystems. Our transect data further revealed that the greatest virus and bacterial abundances are found further into the ablation zone of the Greenland ice sheet at 5–11 km. This implies that our viral and bacterial activity measurements likely do not represent values across the ablation zone, which may

Table 2. Comparative summary of virus production from other sedimentary environments. (Note: B_z (burst sizes) are mean values derived from TEM measurements, values in parentheses are derived from time-course experiments. BDC—bacterial direct counts (mean); VLP—virus like particles; VBR—virus to bacteria ratio; VIBM—virus induced bacterial mortality.)

	Virus counts (10^8 VLP g^{-1})				Virus production (10^8 VLP g^{-1} h^{-1})							
Sediment type	*n*	Range	Median	Mean	*n*	Range	Median	Mean	BDC (10^8 g^{-1})	VBR median	VIBM (%) mean	B_z mean
Freshwater[a]	19	(0.01–203)	10.9	34.2	1	—	0.86	0.86	11.50	4.7	10	46.7
Marine (<100 m)[a]	>20	(0.1–3111)	4.9	89.9	>17	(0.03–1.98)	0.14	0.40	5.00	10	48	15.6
Marine (100–1000 m)[b]	81	(2.4–33.2)	13.1	8.8	81	(0.02–3.34)	0.55	0.80	—	—	64	17(45)
Marine (>1000 m)[a]	14	(0.4–162)	11.6	17.1	4	(0.02–0.70)	0.43	0.43	2.70	5.1	31	20
Marine (>1000 m)[b]	102	(0.5–87.4)	9.2	10.5	102	(0.11–2.75)	0.55	0.62	—	—	89	17(45)
Svalbard cryoconite[c]	3	(5.6–7.5)	6.9	6.7	3	(0.82–0.90)	0.87	0.86	3.92	1.71	>100	2.4
Greenland cryoconite[c]	5	(5.6–15.3)	11.2	10.8	5	(0.44–0.69)	0.57	0.55	3.00	3.38	>100	2.4
GrIS[c]	4	(14.4–24.5)	21.8	20.6	—	—	—	—	13.78	1.63	—	—

[a] (Danovaro *et al* 2008a and references therein) mean values taken from table 1. Median calculated from table 1.

[b] Calculated from supplementary material in Danovaro *et al* (2008b).

[c] This study.

be significantly higher. Especially when considering virus production was correlated with bacterial abundance.

Assuming all viruses produced are from lytic infection of heterotrophic bacteria, viruses were calculated to be responsible for the mean abatement of 598–1710% of all bacterial production in cryoconite holes (using a range of conversion factors for BCP from 10.68 to 30.53 fg C $cell^{-1}$). High values, up to 1500%, have previously been reported from an aquatic hot spring (Breitbart *et al* 2004) which were attributed to Lotka–Volterra, predator–prey relationships between virus and host which may distort single time point measurements such as ours. However, we did not observe such a relationship between viral and bacterial abundances in this study. Bacterial numbers remained relatively unchanged or even slightly increased during the virus production incubations (supplementary figure 1, available at stacks.iop.org/ERL/8/045021/mmedia) which contradicts VIBM values over 100%. There are several factors which could account for these high VIBM values: (1) bacterial carbon production could have been underestimated, either by using incorrect isotopic dilution ratios of leucine in cryoconite bacteria (which is unknown), or the fact that high rates of lysis occurred in the incubations which would release bacterial bound ^{3}H-leucine to dissolved forms making it undetectable by the assay; (2) burst size could have been underestimated as the value calculated for cryoconite holes are the lowest ever reported for sedimentary ecosystems, however they are consistent with other studies in polar aquatic environments (Säwström *et al* 2007, Paterson and Laybourn-Parry 2012). A higher burst size would reduced VIBM estimates, however we also never observed an infected cell with greater than four viruses inside; (3) predator–prey dynamics could have occurred meaning lysis did occur faster than production. As bacterial counts were performed with SYBR gold we could not distinguish between live and dead cells, hence it is possible that recently lysed cells could still be counted and hide a decline in bacterial numbers; (4) other viral life strategies, such as chronic infections, could operate in addition to lysis and account for some of the viruses released. Chronically released virus could be produced without the lysis of the host. However we note the observed high infection frequencies were caused by non-filamentous virus forms. Because of these potential scenarios and the uncertainties in the calculations of virus induced bacterial mortality, we take this measurement to be an estimate of the maximum potential for viral lysis. Thus the production of viruses is a significant process in cryoconite holes, and one which can theoretically account for the lysis of bacterial cells at a rate equivalent to their production or greater. This large scale bacterial lysis and subsequent release of cellular contents has the potential to convert the majority of BCP back into dissolved or colloidal material, reducing its availability for uptake by grazers. This carbon may be less labile after viral lysis but would be at least partially available to the non-infected prokaryotic community. As heterotrophic bacteria are likely to consume a significant proportion of organic carbon from primary production, the high VIBM calculated here implies that the majority of carbon in cryoconite ecosystems flows through viral mediated processes. Hence it is probable that viruses strongly influence the transformation of carbon and nutrients in supraglacial ecosystems. A strong viral shunt is a typical occurrence in the cold, nutrient limited deep sea benthos (table 2 and references therein). Using similar methodology mean VIBM rates have been reported to account for the destruction of approximately 89% of bacterial cell production, decoupling bacterial production from secondary consumers (Danovaro *et al* 2008b). Cryoconite ecosystems are microbially abundant, truncated ecosystems, and whilst grazing rates are unknown, a strong viral shunt implies they are low relative to viral top-down control. A stronger viral shunt may also result in higher rates of bacterial respiration and lower bacterial growth efficiencies, as whilst

DOM is recycled to the heterotrophic community, the overall efficiency of carbon uptake is reduced (Motegi *et al* 2009). Thus the likely dominance of the viral shunt in cryoconite holes may help to explain the high rates of respiration relative to bacterial production previously found in these habitats (Anesio *et al* 2010).

Given the potentially limiting nature of DOC on glacial surfaces, the continued viral mediated release of organic carbon may promote growth in the non-infected microbial community. However, supraglacial ecosystems may be subjected to significant flow of glacial meltwater, which could export DOC to downstream ecosystems. Over the Greenland ice sheet, debris bound organic carbon is significantly less at the marginal sites (sites < 5.4 km from the ice margin) and is negatively correlated with slope (Stibal *et al* 2012b). Recent evidence also suggests dissolved organic matter (DOM) in glacial run off is composed of highly labile carbon and is a significant contributor to bacterial productivity in downstream marine ecosystems (Hood *et al* 2009). Further to this, Hood *et al* (2009) found that this glacial DOM is microbial in origin. Therefore, the virally induced release of organic carbon from cryoconite bound bacteria could enhance its export from supraglacial environments and stimulate microbial communities in hydrologically connected ecosystems.

Acknowledgments

This research was funded by the UK Natural Environmental Research Council (NERC—NE/G00496X/1) to AMA and the Leverhulme Trust (RPG-2012-624) to AMA and CMB. CMB was also funded by a NERC Doctoral Training Programme grant. We would like to thank staff at the NERC Arctic Research Station and Kangerlussuaq International Science Support for logistical support and field assistance. We would also like to thank two anonymous reviewers for valuable comments to an earlier draft of this letter.

References

Anesio A M, Hodson A J, Fritz A, Psenner R and Sattler B 2009 High microbial activity on glaciers: importance to the global carbon cycle *Glob. Change Biol.* **15** 955–60

Anesio A M, Mindl B, Laybourn-Parry J, Hodson A J and Sattler B 2007 Viral dynamics in cryoconite holes on a high Arctic glacier (Svalbard) *J. Geophys. Res.* **112** G04S31

Anesio A M, Sattler B, Foreman C, Telling J, Hodson A, Tranter M and Psenner R 2010 Carbon fluxes through bacterial communities on glacier surfaces *Ann. Glaciol.* **51** 32–40

Bettarel Y, Bouvy M, Dumont C and Sime-Ngando T 2006 Virus–bacterium interactions in water and sediment of West African inland aquatic systems *Appl. Environ. Microbiol.* **72** 5274–82

Breitbart M, Wegley L, Leeds S, Schoenfeld T and Rohwer F 2004 Phage community dynamics in hot springs *Appl. Environ. Microbiol.* **70** 1633–40

Danovaro R, Corinaldesi C, Filippini M, Fischer U R, Gessner M O, Jacquet S, Magagnini M and Velimirov B 2008a Viriobenthos in freshwater and marine sediments: a review *Freshwater Biol.* **53** 1186–213

Danovaro R, Dell'Anno A, Corinaldesi C, Magagnini M, Noble R, Tamburini C and Weinbauer M 2008b Major viral impact on the functioning of benthic deep-sea ecosystems *Nature* **454** 1084–8

Fountain A G, Tranter M, Nylen T H, Lewis K J and Mueller D R 2004 Evolution of cryoconite holes and their contribution to meltwater runoff from glaciers in the McMurdo Dry Valleys, Antarctica *J. Glaciol.* **50** 35–45

Hodson A, Anesio A M, Tranter M, Fountain A, Osborn M, Priscu J, Laybourn-Parry J and Sattler B 2008 Glacial ecosystems *Ecol. Monogr.* **78** 41–67

Hodson A, Cameron K, Bøggild C, Irvine-Fynn T, Langford H, Pearce D and Banwart S 2010 The structure, biological activity and biogeochemistry of cryoconite aggregates upon an Arctic valley glacier: Longyearbreen, Svalbard *J. Glaciol.* **56** 349–62

Hodson A *et al* 2007 A glacier respires: quantifying the distribution and respiration CO_2 flux of cryoconite across an entire Arctic supraglacial ecosystem *J. Geophys. Res.* **112** G04S36

Hood E, Fellman J, Spencer R G M, Hernes P J, Edwards R, D'Amore D and Scott D 2009 Glaciers as a source of ancient and labile organic matter to the marine environment *Nature* **462** 1044–7

Loferer-Krößbacher M, Klima J and Psenner R 1998 Determination of bacterial cell dry mass by transmission electron microscopy and densitometric image analysis *Appl. Environ. Microbiol.* **64** 688–94

Mei M L and Danovaro R 2004 Virus production and life strategies in aquatic sediments *Limnol. Oceanogr.* **49** 459–70

Motegi C, Nagata T, Miki T, Weinbauer M G, Legendre L and Rassoulzadegan F 2009 Viral control of bacterial growth efficiency in marine pelagic environments *Limnol. Oceanogr.* **54** 1901–10

Noble R T and Fuhrman J A 1997 Virus decay and its causes in coastal waters *Appl. Environ. Microbiol.* **63** 77–83

Paterson H and Laybourn-Parry J 2012 Antarctic sea ice viral dynamics over an annual cycle *Polar Biol.* **35** 491–7

Porazinska D L, Fountain A G, Nylen T H, Tranter M, Virginia R A and Wall D H 2004 The biodiversity and biogeochemistry of cryoconite holes from McMurdo Dry Valley glaciers, Antarctica *Arct. Antarct. Alp. Res.* **36** 84–91

Posch T, Loferer-Krößbacher M, Gao G, Alfreider A, Pernthaler J and Psenner R 2001 Precision of bacterioplankton biomass determination: a comparison of two fluorescent dyes, and of allometric and linear volume-to-carbon conversion factors *Aquat. Microb. Ecol.* **25** 55–63

Säwström C, Granéli W, Laybourn-Parry J and Anesio A M 2007 High viral infection rates in Antarctic and Arctic bacterioplankton *Environ. Microbiol.* **9** 250–5

Säwström C, Mumford P, Marshall W, Hodson A and Laybourn-Parry J 2002 The microbial communities and primary productivity of cryoconite holes in an Arctic glacier (Svalbard 79°N) *Polar Biol.* **25** 591–6

Smith D C and Azam F 1992 A simple, economical method for measuring bacterial protein synthesis rates in seawater using ^{3}H-leucine *Mar. Microb. Food Webs* **6** 107–14

Sømme L 1996 Anhydrobiosis and cold tolerance in tardigrades *Eur. J. Entomol.* **93** 349–57

Stibal M, Šabacká M and Kaštovská K 2006 Microbial communities on glacier surfaces in Svalbard: impact of physical and chemical properties on abundance and structure of cyanobacteria and algae *Microb. Ecol.* **52** 644–54

Stibal M, Šabacká M and Žárský J 2012a Biological processes on glacier and ice sheet surfaces *Nature Geosci.* **5** 771–4

Stibal M, Telling J, Cook J, Mak K M, Hodson A and Anesio A M 2012b Environmental controls on microbial abundance and activity on the Greenland ice sheet: a multivariate analysis approach *Microb. Ecol.* **63** 74–84

Suttle C A and Chen F 1992 Mechanisms and rates of decay of marine viruses in seawater *Appl. Environ. Microbiol.* **58** 3721–9

Telling J, Anesio A M, Tranter M, Stibal M, Hawkings J, Irvine-Fynn T, Hodson A, Butler C, Yallop M and Wadham J 2012 Controls on the autochthonous production and respiration of organic matter in cryoconite holes on high Arctic glaciers *J. Geophys. Res.* **117** G01017

Theil-Nielsen J and Søndergaard M 1998 Bacterial carbon biomass calculated from biovolumes *Arch. Hydrobiol.* **141** 195–207

Weinbauer M G and Suttle C A 1996 Potential significance of lysogeny to bacteriophage production and bacterial mortality in coastal waters of the Gulf of Mexico *Appl. Environ. Microbiol.* **62** 4374–80

Wharton R A, McKay C P, Simmons G M and Parker B C 1985 Cryoconite holes on glaciers *Bioscience* **35** 499–503

Wilhelm S W and Suttle C A 1999 Viruses and nutrient cycles in the sea *Bioscience* **49** 781–8